UNIVERSITY OF AGDER

ENE-503 Energy Research Project

SIMULATING THE THERMAL POTENTIAL FOR ENERGY STORAGE IN AN ELECTRIC WATER HEATER TANK

BY

AMUND RUUD HVAL

SUPERVISOR:
GUNSTEIN SKOMEDAL

This master's thesis is carried out as a part of the education at the University of Agder and is therefore approved as a part of this education. However, this does not imply that the University answers for the methods that are used or the conclusions that are drawn.

UNIVERSITY OF AGDER, 2017

FACULTY OF TECHNOLOGY AND SCIENCE

DEPARTMENT OF ENGINEERING

Abstract

This thesis uses a CFD model of an electric water heater tank(EWHT) to investigate the stratification in the tank during different discharge experiments. Stratification in a tank happens naturally as hot water rises to the top and cold water sinks to the bottom, due to the difference in density of the water based on the temperature. The simulation found that for higher discharges the stratification becomes better and it is possible to extract more hot water from the tank than at lower discharges. Although the simulation built in this study can simulate all operations of the tank separately, it has not been successful to build a model that can simulate all operations in the same study.

I

Preface

I would like to thank my supervisor Dr. Gunstein Skomedal for help and guidance during this project. I would also like to thank Johan Olav Brakestad for invaluable help when assembling the experimental tank. Lastly, I would like to thank Marius Christoffersen for the collaboration while building and setting up the testing environment for the experimental tank. I also appreciate the support from Professor Anne Gerd Imenes and Dr. Charly Berthod during this project.

Amund Ruud Hval

Grimstad, May 31, 2018

Individual declaration

The individual student or group of students is responsible for the use of legal tools, guidelines for using these and rules on source usage. The statement will make the students aware of their responsibilities and the consequences of cheating. Missing statement does not release students from their responsibility.

1.	I hereby declare that my thesis is my own work and that I/We have not used any other sources or have received any other help than mentioned in the thesis.	☑
2.	I further declare that this thesis: - not been used for another exam at another department/university/university college in Norway or abroad; - does not refer to the work of others without it being stated; - does not refer to own previous work without it being stated; - have all the references given in the literature list; - is not a copy, duplicate or copy of another's work or manuscript.	☑
3.	I am aware that violation of the above is regarded as cheating and may result in cancellation of exams and exclusion from universities and colleges in Norway, see Universitets- og høgskoleloven §§4-7 og 4-8 og Forskrift om eksamen §§ 31.	☑
4.	I am aware that all submitted theses may be checked for plagiarism.	☑
5.	I am aware that the University of Agder will deal with all cases where there is suspicion of cheating according to the university's guidelines for dealing with cases of cheating.	☑
6.	I have incorporated the rules and guidelines in the use of sources and references on the library's web pages.	☑

Publishing Agreement

Authorization for electronic publishing of the thesis.	
Author(s) have copyrights of the thesis. This means, among other things, the exclusive right to make the work available to the general public (Åndsverkloven. §2). All theses that fulfill the criteria will be registered and published in Brage Aura and on UiA's web pages with author's approval. Theses that are not public or are confidential will not be published.	
I hereby give the University of Agder a free right to make the task available for electronic publishing:	YES ☑ NO ☐
Is the thesis confidential? (confidential agreement must be completed)	YES ☐ NO ☑
- If yes: Can the thesis be published when the confidentiality period is over?	YES ☐ NO ☐
Is the task except for public disclosure? (contains confidential information. see Offl. §13/Fvl. §13)	YES ☐ NO ☑

Contents

List of Figures

List of Tables

List of Symbols

Abbreviations

CFD   Computational Fluid Dynamics

EWHT Electric Water Heater Tank

PV   Photovoltaic

Symbols

A Area

c_p Specific heat

D Diameter

E Energy

E_R Energy response factor

f Force

g Gravitational acceleration

H Height

k Thermal conductivity

L Length

$\dot{m}$ Mass flow rate

m Mass

M_E Moment of energy

MIX MIX number

P Pressure

$\dot{q}$ Heat transferred

$\dot{S}$ Entropy generation

S Entropy

s Specific entropy

T Temperature

t Time

U Velocity

u Velocity in x-direction

$\dot{V}$ Volume flow rate

V Volume

v Velocity in y-direction

w Velocity in z-direction

α Thermal diffusivity

β Volume thermal expansion coefficient

μ Dynamic viscocity

ν Kinematic viscocity

ξ Exergy

ρ Density

τ Shear stress

1   Introduction

As photovoltaic(PV) installations become more widespread more and more energy will be produced during the middle of the day, while the peak consumption times are during the morning and evening when PV installations will produce less power. For private household installations, selling the excess power produced is not economical compared to using it. Since there are some extra costs to buying electricity over the electricity price that is not paid when the customer is selling electricity. To combat this, the power needs to be stored instead of sold to be able to use this electricity at a later time. To store power locally the natural choice would be a battery, but this has a significant capital cost. Another alternative is to use an electric water heater tank (EWHT). Most houses already have an EHWT installed, and it could be possible to store energy without much extra investment, such as would be the case with batteries. To be able to store energy, the tank would need not to be saturated when the PV panels produce electricity. Most EWHTs operate with the parameters that when hot water is used the heating element starts heating the water in the tank back up to a set temperature. To be able to store the excess power produced by the PV system the heating element would have to be controlled in such a way that it not automatically starts heating the water if there is possible to delay the heating until the solar power can produce excess electricity. To accomplish this, the thermal properties of the tank should be investigated.

During normal operation of the tank stratification will occur in the tank, this means that the temperature in the water of the tank will have different temperatures as hot water will rise to the top and cold water fall to the bottom due to the difference in density of water based on temperature. If the tank were used as a battery, this effect would have to be accounted for. The stratification in the tank means that the water in the top of the tank would be warmer than what would be the case in a tank with uniform temperature. A tank with better stratification could deliver more hot water. When using an intermittent energy source such as the sun, which is affected by time of day and the clouds, a tank that can be used for longer without heating would be preferable

The water flow into the EWHT will be affected by the pressure in the water mains both locally in the household as well as regionally. The water pressure coming into the house will be affected both by how much water is used in the area as well as the levels of the reservoirs supplying an area. When the water reaches the house, the pressure could still be affected by how much water is used in the household, and if many points in the house are trying to extract water at the same time, the water pressure will be lower than if only one point in the house uses water. Because of this different flow rates into the tank has been tested and their effect on stratification has been studied.

1.1   Problem statement

This thesis will introduce a computation fluid dynamics (CFD) model to simulate the operations of a real EWHT. The model of the tank will be built and verified against experimental data from an EWHT installed at the University of Agder. The model has been used to investigate different characteristics of the tank, namely the effect of changing the flow rate into the tank.

The thesis will be divided into two parts:

- Building a CFD model and using experimental data to verify the simulation

- Investigate changing inflow rate and its effect on stratification.

1.2   Report Structure

- **1   Introduction**
  This section presents the problem statement and motivation of the thesis

- **2   Theory**
  Here the different ways to model the tank and the theory behind CFD modeling is introduced. Finally the literature written to describe the stratification in hot water storage has been reviewed.

- **3   Method**
  The method used to model the tank in COMSOL and verify it with experimental data from a real tank is presented. Also the formulas used to compare the stratification in the tank is expressed.

- **4   Results**
  In the result section the results from the validation of the model is presented, and the results from the study of the different mass flow rates.

- **5   Discussion** In this section the results are discussed, in addition the experimental tank has been checked against design parameters suggested in the literature for better stratification.

- **6   Conclusion**
  Presents the conclusion of the thesis

- **7   Further Work**
  Suggestions for further study with the experimental tank.

2   Theory

This section presents the theory behind computational fluid dynamics, and also a review of the literature concerning stratification in the experimental tank. Some of the theory presented concerning stratification was written in an earlier pre project[1]

2.1   Modelling a Thermal Energy Storage

Numerous processes are affecting the tank at any given time. Heat losses to the surrounding, heat transfer between the different temperature layers, mixing due to inlet flow to name a few. Taking all the processes into account, the equations needed are complicated to solve mathematically. It has therefore over the years been developed different models to simulate the water tank. Dumont et al. [2] classified different models used to model thermal energy storage into eight categories: analytical, fully mixed, blackbox, moving boundary, plug flow, multinode, zonal and CFD. Some of these models are illustrated in figure 1
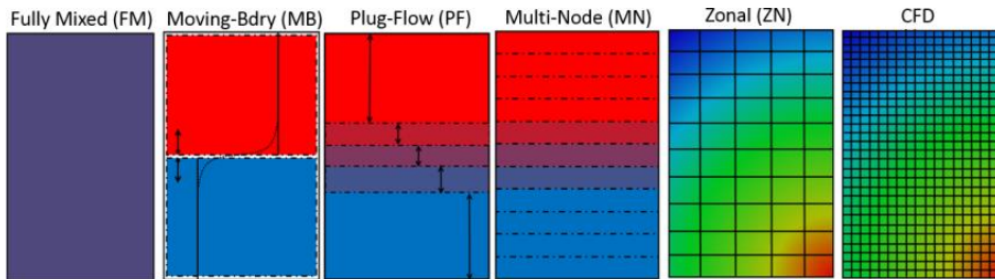
Figure 1 – Different methods to model temperature distribution in hot water storage, from [2, Figure 2].

The analytical model describes the system with analytical functions, and today these models are mostly used to model ideally stratified or fully mixed tanks [3]. A comparison of older analytical models can be found in Zurigat et al. [4]. The fully mixed model considers the tank as having equal temperature through the whole tank. For stratification purposes, this is too much of a simplification to be useful.

The blackbox model considers the tank as a black box and uses a database that can give an output for any given input. This means that the model would need extensive experimental data or multiple CFD simulations to generate the data needed to use it. The moving boundary model uses an ideal thermocline (i.e., the thermocline has zero thickness) to divide the tank into two regions (hot and cold). The volume of each region is changed by moving the thermocline. One such model has been developed by Dickes et al. [5].

The plug flow model [6, 7] is a model often used for charge or discharge experiments. The water is divided into different discs based on temperature. When water flows into the tank, this is represented with a new disc with the volume of the water inserted. In this model, discs would also be combined if the temperature difference is below a certain threshold. The multi-node model [8, 9] is similar to the plug-flow model, with the tank divided into different discs, but in

this model, the size of the discs are equal and constant, and no new discs are inserted during the experiment.

The zonal and CFD model both uses a 3D mesh to model the tank. The volume of the tank is divided into smaller volumes and then uses differential equations to solve each one. The zonal model uses a large mesh, and this means the computational time is shorter, but it is not as precise as CFD. CFD is the most exact model used today, the drawback of the model is that the simulation could be time-consuming and for long simulations such as annual, a simple model should be chosen [10]. CFD models have been used extensively in the literature, especially in the last years [11–14].

Of the modesl presented in this section the most exact model is CFD, followed by zonal. But these models could be time-consuming, they also require expensive software. Often the plug-flow or multi-node model could be used with satisfactory results.

2.2 CFD

The mathematics that governs CFD is based on the equations of fluid dynamics, namely the conservation of mass, momentum, and energy.

2.2.1 Mass Conservation

The mass conservation law states that the mass of a system if it is closed to all transfer of mass or energy, must remain constant. The equation for mass conservation is,

$$\frac{\partial \rho}{\partial t} + \frac{\partial (\rho u)}{\partial x} + \frac{\partial (\rho v)}{\partial y} + \frac{\partial (\rho w)}{\partial z} = 0 \,, \tag{1}$$

where ρ is the density, t is the time and u, v and w are the velocity in the x, y and z components respectively. For an incompressible fluid, the density(ρ) is constant, and the equation becomes,

$$\frac{\partial (u)}{\partial x} + \frac{\partial (v)}{\partial y} + \frac{\partial (w)}{\partial z} = 0 \,. \tag{2}$$

2.2.2 Momentum Conservation

The conservation of momentum is Newton's Second Law given as $F = ma$. The forces acting on an object is given as the mass times the acceleration of the object. The momentum equation can be given in x, y, and z-direction as,

$$\rho \frac{Du}{Dt} = -\frac{\partial P}{\partial x} + \frac{\partial \tau_{xx}}{\partial x} + \frac{\partial \tau_{yx}}{\partial y} + \frac{\partial \tau_{zx}}{\partial z} + \rho f_x \,, \tag{3}$$

$$\rho \frac{Dv}{Dt} = -\frac{\partial P}{\partial y} + \frac{\partial \tau_{xy}}{\partial x} + \frac{\partial \tau_{yy}}{\partial y} + \frac{\partial \tau_{zy}}{\partial z} + \rho f_y \,, \tag{4}$$

$$\rho \frac{Dw}{Dt} = -\frac{\partial P}{\partial z} + \frac{\partial \tau_{xz}}{\partial x} + \frac{\partial \tau_{yz}}{\partial y} + \frac{\partial \tau_{zz}}{\partial z} + \rho f_z \,, \tag{5}$$

where P is the pressure, τ is the shear stresses and f is the forces.

UNIVERSITY OF AGDER

2.2.3 Energy Conservation

Then conservation of energy is given by the first law of thermodynamics, stating that the rate of heat change for a system is equal to the rate of heat addition plus the rate of work done. The equation for energy conservation is,

$$
\begin{aligned}
\rho \frac{D}{Dt}(e + \frac{U^2}{2}) = \rho\dot{q} &+ \frac{\partial}{\partial x}(k\frac{\partial T}{\partial x}) + \frac{\partial}{\partial y}(k\frac{\partial T}{\partial y}) + \frac{\partial}{\partial z}(k\frac{\partial T}{\partial z}) \\
&- \frac{\partial(uP)}{\partial x} - \frac{\partial(vP)}{\partial y} - \frac{\partial(wP)}{\partial z} + \frac{\partial(u\tau_{xx})}{\partial x} \\
&+ \frac{\partial(u\tau_{yx})}{\partial y} + \frac{\partial(u\tau_{zx})}{\partial z} + \frac{\partial(v\tau_{xy})}{\partial x} + \frac{\partial(v\tau_{yy})}{\partial y} \\
&+ \frac{\partial(v\tau_{zy})}{\partial z} + \frac{\partial(w\tau_{xz})}{\partial x} + \frac{\partial(w\tau_{yz})}{\partial y} + \frac{\partial(w\tau_{zz})}{\partial z} + \rho\boldsymbol{f}\cdot\boldsymbol{U} \,, \quad (6)
\end{aligned}
$$

where U is the velocity, $\dot{q}$ is the heat transferred, k is the thermal conductivity and $\boldsymbol{f}\cdot\boldsymbol{U}$ is the dot product of the velocity and force vector.

2.2.4 Boundary conditions

While the equation above governs the flow in the system, the system is defined by boundary conditions. The boundary conditions dictate the solutions for a system from the governing equations. Some of the most common boundary conditions are; inlet/outlet, wall, constant pressure, symmetry, and periodicity.[15]

The inlet/outlet boundary condition describes the surface where fluid enters and leaves the computational domain. The typical conditions used for this are velocity, pressure or mass flow of the fluid.

The wall boundary is the most common boundary condition in a CFD simulation and describes a domain that is impenetrable for the fluid. For most solid walls a 'no-slip' boundary condition is used. This describes the velocity of the fluid on the wall, and for the 'no-slip condition says that the fluid at the boundary is zero ($u = v = w = 0$).

The constant pressure boundary describes a point in the computational domain where the pressure is known and is constant. Thes boundary is mostly used for places where the domain is open to the environment, and there is atmospheric pressure.

The symmetric boundary can be used to cut down on computational time in systems where the flow is symmetrical, and therefore only half of the system is needed for computing the results.

The periodic or cyclic boundary also takes advantage of symmetry in a system. Where the flow has a periodic symmetry, easier computations can be done by knowing that the flow is the same after a given period, for instance with a propeller or other swirling flows.
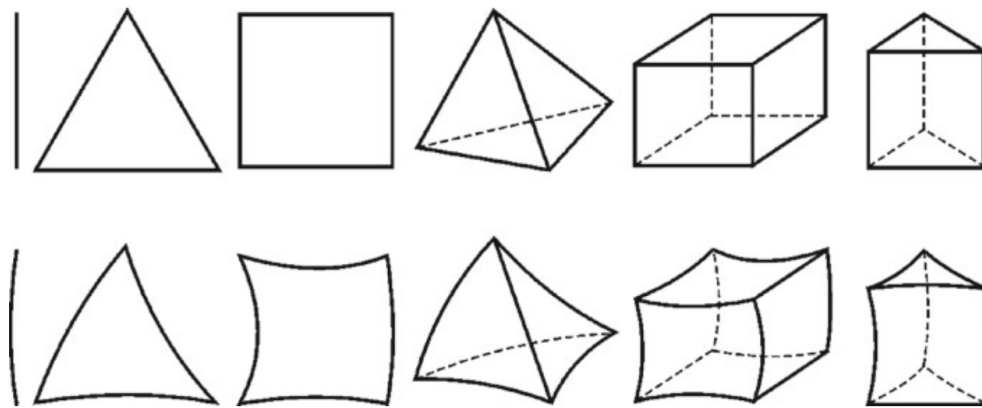
Figure 2 – Typical grid cells from [16, Figure 1.1]

2.2.5 Discretization and mesh

To solve a CFD problem, the governing equations must be discretized. The equations used has an infinite continuum of values in the domain, and discretization expresses the equations such that it only gives values for a finite number of discrete points in the domain. The method used to solve the problem decides how the equations are discretized, the most common methods are the Finite Difference Methode(FDM), Finite Volume Methode(FVM) and Finite Element Methode(FEM). COMSOL uses FEM to solve CFD problems, and this is the method that will be discussed here.

For FEM modeling the domain is divided into a set of volumes or finite elements, and the conservation equations are applied for each element. The equations are then multiplied by a weight function for each element before being integrated over the entire domain.

To use FEM the geometry must be divided into finite elements, and this in CFD is called a mesh. In figure 2 the most standard cells used to mesh a geometry is shown. In 1D the mesh is a simple line as shown first in the figure. For 2D geometries, triangles and quadrilaterals are used. Finally, for 3D geometries, the most used are tetrahedrons and hexahedron, and some applications also use prisms and pyramids. These cells are then mapped onto the geometry to cover the whole geometry so that the program can solve the problem with discretization. When meshing it is important to find the right mesh to use. Too fine a mesh with too many elements will give a very computational heavy calculation that will take a long time to compute. If the mesh is too coarse, the results might not be correct as there is too much difference in values within one element.

2.3 Dimensionless numbers

Some dimensionless numbers used in the modelling of a stratified water tank will be briefly explained in this section.

The Reynolds number (Re) describes the flow due to forced convection. For high Reynolds

numbers the flow is turbulent (Re>4000) and for lower numbers (Re<4000) the flow is laminar.

$$Re = \frac{\rho U L}{\mu} \,, \tag{7}$$

where L is the characteristic length and μ is the dynamic viscosity of the fluid.

The Grashof number (Gr) describes the ratio of buoyancy to viscous forces acting on a fluid,

$$Gr = \frac{L^3 g \beta \Delta T}{\nu} \,, \tag{8}$$

where g is gravitational acceleration, β is the volume thermal expansion coefficient of the fluid, ΔT is the temperature difference and ν is the kinematic viscosity of the fluid.

The modified Richardson number (Ri) represents natural convection relative to forced convection,

$$Ri = \frac{Gr}{Re^2} \,. \tag{9}$$

For very low values of Richardson number (e.g. $Ri < 0.1$) natural convection is negligible, while for high Richardson numbers (e.g $Ri > 10$) forced convection will be negligible.

The Péclet number (Pe) expresses the ratio of convective heat transfer by the fluid, to conductive heat transfer,

$$Pe = \frac{U L}{\alpha} \,, \tag{10}$$

where α is the thermal diffusivity of the fluid.

The Fourier number (Fo) expresses the ratio of heat transfer due to conduction, to the heat accumulated in the system,

$$Fo = \frac{\alpha t}{L} \,. \tag{11}$$

The Rayleigh Number (Ra) describes the free convective heat transfer along a surface. The Rayleigh number can indicate if flow due to natural convection is laminar or turbulent. For a vertical cylinder the flow is laminar for $Ra < 10^8$ and fully turbulent for $Ra > 10^{10}$. The Rayleigh number is expressed as,

$$Ra = \frac{g \beta \Delta T D^3}{\nu \alpha} \,. \tag{12}$$

2.4 Stratification

Thermal stratification develops because water at different temperature has different density. Hot water has a lower density than cold water will rise to the top. Thermal stratification will happen naturally in a water tank that does not have a heat source and have a higher temperature than the environment. Figure 3 has a graphical representation of stratification in thermal storage. As can be seen from this figure, at the same energy level, a stratified tank will have water with a higher temperature in the top of the tank compared to the fully-mixed tank.

(a) The ideally stratified tank

(b) The experimental tank

(c) The fully mixed tank
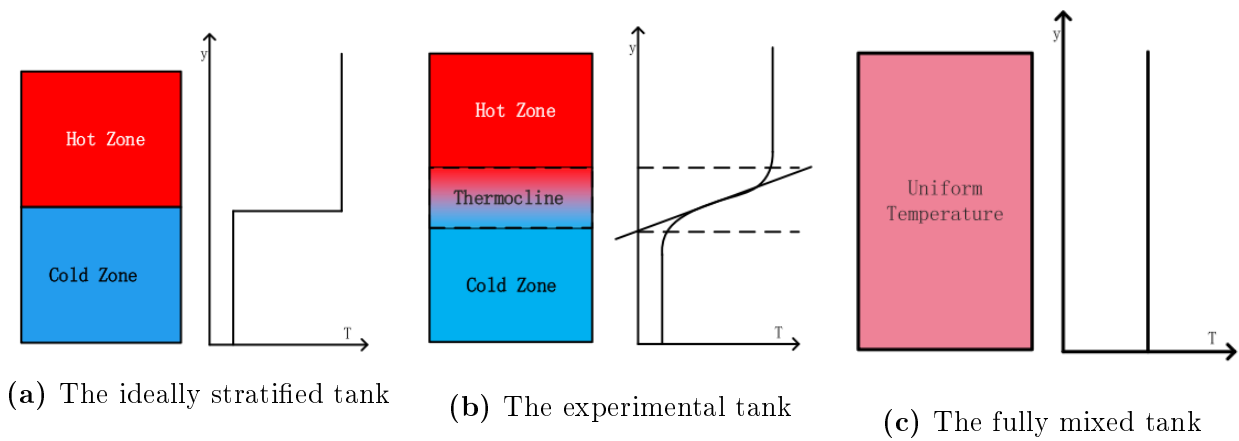
Figure 3 – Degrees of stratification in a tank with the same energy, from [14, Figure 6].

The thermocline shown in the figure is the point in the tank were the temperature changes more rapidly than other parts of the tank. The hot and cold zone will also have some stratification, but the temperature difference will be smaller. The thinner the thermocline is, the better the stratification. Comparing the ideally stratified tank (figure 3a) with the fully mixed tank (figure 3c), when extracting water from the fully mixed tank, the temperature in the whole tank would decrease, assuming an inlet temperature below the temperature of the tank. In an ideally stratified tank when extracting water, instead of changing the temperatures in the tank, the size of the hot and cold zone would change, assuming inlet temperature equal to the cold zone. Using the stratified tank we are then able to extract water at the same temperature instead of water that becomes colder as more water is extracted. Cristofari et al. [17] found that by inducing stratification in a tank, there was possible to increase the energy output from solar collectors by 5.25 % compared to using a fully-mixed tank.

The phenomena of stratification in nature have been studied since the early 20th century [18, 19]. However, it was not until the early 1970's that stratification was studied in thermal storage [20]. This section introduces a review of the literature concerning stratification in thermal storage. Both the physical properties of the tank that impact the stratification and the methods that have been used to simulate a stratified water tank have been reviewed. Much of the literature concerning thermal stratification has been done considering solar thermal systems, in this study only the parts that can be translated to an electric water heater are considered.

2.4.1 The Influence of Tank Geometry on Thermal Stratification

Yang et al. [21] studied different tank geometries and their effect on stratification. In this study, ten different tank shapes are investigated, comparing their impact on thermal energy and exergy storage capacity, and the tank stratification. It was found that for shapes with sharp corners such as two cones placed against each other the stratification was highest, and for shapes with flat tops and bottoms such as a cylinder or barrel the stratification was lowest. For exergy and energy storage capacity a barrel or sphere shape was the best and cylinder was the worst. Other factors than the shape also contribute to the stratification in a tank: the height/diameter (H/D) ratio, the inlet/outlet flow and obstacles inside the tank. These factors

are described further below.

H/D ratio

The first experiment on the ratio between height and diameter of a hot water storage tank was performed by Lavan and Thompson [22]. They concluded that stratification increases with increasing H/D. From looking at cost versus performance, they found a ratio between 3 and 4 to be most reasonable. Khalifa et al. [23] also found experientially that the stratification increases with higher H/D ratios, while Ismail et al. [24] and Hahne et al. [25] found by modeling that for ratios higher than 4, the effect of increased stratification became negligible.

Tank Inlets

Dependent on how much turbulence is created by the flow of water into a tank, a region in the tank will mix the temperature layers. To maintain stratification, the tank inlet and the inlet flow should be designed so that this mixing region is as small as possible. Moncho-Esteve et al. [12] tested two different inlet designs, an elbow design and a diffuser design. Elbow is 90 degrees bent inlet design. A diffuser is an inlet design were the water exits through many small holes. It was found that stratification was more affected by inlet direction and inlet velocity rather than inlet design, but the diffuser did provide better results than the elbow design. Zurigat et al. [26] tested different diffuser designs and found only small differences between the designs. A study of the position of the tank was done by Bouhdjar et al. [27]. They found that the best position of the inlet and outlet was at the bottom and top of the tank. Lavan and Thompson [22] found that moving the inlet just one inch above from the bottom of the tank, would decrease the stratification. Moving the outlet was found to be much less crucial.

Obstacles inside the tank

Aluntop et al. [28] did an extensive study of obstacles inside a tank with horizontal inlets. They found that any obstacle placed near the bottom of the tank will increase stratification. The obstacle stops the flow upwards containing the mixing below the obstacle. It was found that obstacles that lead the water through the middle of a tank, away from the sides will produce the best stratification. Aviv et al. [29] tested putting a baffle in front of a vertical inlet. It was found that for small discharges (2 and 3 l/min) there was only a small effect of the baffle. For higher flow rates (5 and 7 l/min) the baffle prevented mixing in the higher parts of the tank. The experiments were also tested with two baffles, but this did not give better results than one baffle.

Stratification Efficiency

Many methods have been developed to describe the stratification in a thermal storage tank. The stratification efficiency by itself does not reveal much, but it can be used to compare different discharge regiments and compare different tank designs. Rosen et al. [30] pointed out that," *no generally valid basis for comparing the achieved performance of one storage with that of another operating under different conditions has found broad acceptance.*"

Lavan and Thompson [22] used an extraction efficiency $\eta_e = \dot{V}t^*/V$, where t^* is the dimensionless time at which the difference between the initial inlet and outlet temperature has dropped below a certain percent, here 10% ($\Delta T_{end} = 0.10\Delta T_{start}$). $\dot{V}$ is volume flow rate and V is the volume of the tank. Using experimental data Lavan and Thompson was able to correlate the data with dimensionless numbers to find a new equation for the efficiency based on the inlet Reynolds number (Re_d), Grashof number (Gr_D) and height/diameter (H/D) ratio, see equation 13,

$$\eta = 1 - \exp\left(-0.067Re_d^{-0.55}Gr_D^{0.35}(H/D)^{0.58}\right). \tag{13}$$

It was found that a low Reynolds number and a high H/D ratio would give the best stratification, and as mentioned in section 2.4.1, the position of the inlet also contributed to the stratification. Lavan and Thompson were the first to look at discharge or charging efficiency to represent the stratification by correlating it to dimensionless numbers. Later studies have also worked on this, for instance Hanhe et al. [25]. This study used a charging efficiency to measure the stratification in the tank,

$$\eta_c = \frac{\int_0^{t_c} \dot{m}c_p[T_{in} - T_o(t)]dt}{mc_p(T_{in} - T_{ini})}, \tag{14}$$

where $\dot{m}$ is the charging mass flow rate of water, m is the mass of water in the tank, c_p is the specific heat of water and T_{in}, T_o and T_{ini} is the inlet, outlet and initial water temperature, respectively. As Lavan and Thompson, Hanhe et al. also correlated the data with dimensionless numbers to find a new expression for the equation based on the modified Richardson number (Ri), Peclet number (Pe), Fourier number (Fo) and H/D ratio

$$\eta_c = 1 - 0.206Ri_{H,f}^{-0.57}Pe_{H,f}^{-0.49}Fo_{H,f}^{-0.74}(H/D)^{-1.1}. \tag{15}$$

Davidson et al. [8] defined a MIX number based on the moment of energy. The MIX number of 0 represents an ideally stratified tank and a MIX number of 1 represents a fully-mixed tank. Moment of energy was calculated as

$$M_E = \sum_{i=1}^n y_i E_i, \tag{16}$$

where y_i is the height from the bottom of the tank to the middle of node i and E_i is the energy in node i calculated as

$$E = mc_p\Delta T. \tag{17}$$

The MIX number is then calculated as

$$MIX = \frac{(M_{E,str} - M_{E,actual})}{(M_{E,str} - M_{E,mix})}, \tag{18}$$

where the subscripts represent an ideally stratified tank ($M_{E,str}$), the actual value in the tank ($M_{E,actual}$), and a fully mixed tank ($M_{E,mix}$).

The studies reviewed so far are based on energy in the tank or the first law of thermodynamics. Other studies have argued for using the exergy* (second law of thermodynamics) or entropy[†] (combined first and second law) instead to represent the stratification in the tank. Rosengarten et al. [31] defined a stratification efficiency (η_{st}) as a ratio of stored exergy to stored energy.

$$\eta_{st} = \frac{\xi}{mc_p(T_{del} - T_{mean})} = 1 - \frac{T_a}{H(T_{del} - T_{mean})} \int_0^H ln\left(\frac{T_{del}}{T(y)}\right) dy\,, \qquad (19)$$

where ξ is the exergy, H is the height of the tank and T_y,T_{mean} and T_a is the temperature at height y, mean temperature in the tank and ambient temperature, respectively. T_{del} is the reference temperature, since exergy is the energy in the system able to do work a reference temperature must be chosen where the energy is not able to do work. In the study of Rosengarten et al. this is defined as the delivery temperature, this is the lowest temperature the system should output when delivering hot water. This efficiency was compared to an older energy efficiency method, which compared the energy in the tank to the energy in a mixed tank. The results showed that the stratification efficiency of Rosengarten et al. better represented the stratification in the tank. Rosen et al. [30] used an expression for the exergy (ξ) in the storage to the fully mixed exergy (ξ_m) in the same storage.

$$\frac{\xi}{\xi_m} = \frac{T_e/T_a - 1 - ln(T_e/T_a)}{T_m/T_a - 1 - ln(T_m/T_a)}\,, \qquad (20)$$

where T_e is the equivalent temperature of a fully mixed storage with the same exergy as the real storage and T_m is the temperature if the real storage was mixed. The ambient temperature is what is used as reference temperature in this method. T_e and T_m is not the same since it was found that the exergy would increase with increased stratification even if the energy was the same. This means a mixed storage with the same exergy compared with the real storage would have higher energy.

Shah and Furbo [32] used a exergy efficiency and a entropy efficiency comparing the actual situation to the ideal situation

$$\eta_s = \frac{(S_0 - S_1)_{ideal}}{(S_0 - S_1)_{actual}} \qquad \eta_\xi = \frac{\xi_{1-0,actual}}{\xi_{1-0,ideal}}\,, \qquad (21)$$

where $(S_0 - S_1)$ is the entropy change, and ξ_{1-0} is the exergy change. These expressions are calculated as

$$(S_o - S_1) = mc_p ln\left(\frac{T_0}{T_1}\right) \qquad \xi_{1-0} = c_p\left[m(T_1 - T_0) + mT_0 \cdot ln\left(\frac{T_0}{T_1}\right)\right]\,, \qquad (22)$$

T_1 is the temperature in the tank and T_0 is the temperature when the tank is at dead state and is here used as the reference temperature. Shah and Furbo used this method during discharge

---

*Exergy is defined as the energy in the system that can do work. In the case of a water heater this is the energy in the tank that can be used as hot water.
[†]Entropy is the ratio of added heat to the absolute temperature at which it was added

experiments and for this dead state was chosen to be when the whole tank had the same temperature as the inlet temperature.

Panthalookaran et al. [33] developed a storage evaluation number based on the entropy generation ($\dot{S}$) and the energy response factor (E_R), which is a factor for the change in energy during a process compared to an ideal change in energy(no mixing, only heat loss to the environment). They proposed two numbers, one for charging and discharging (η_{SEN1}) and one for storing (η_{SEN2})

$$\eta_{SEN1} = \left[1 - \frac{\dot{S}}{E_R}\right] \qquad \eta_{SEN2} = \left[1 - \dot{S}E_R\right], \qquad (23)$$

where

$$\dot{S} = \frac{\Delta S_{real} - \Delta S_{stratified}}{\Delta S_{mixed} - \Delta S_{stratified}} \qquad and \qquad E_R = \frac{\Delta E_{real,s}}{\Delta E_{ideal,s}}, \qquad (24)$$

here

$$\Delta S = \int_V \rho \Delta s_{1-2} dV = \int_V \rho c_p ln(\frac{T2}{T1}) dV \qquad and \qquad \Delta E = m c_p (T2 - T1), \qquad (25)$$

where ΔS is the change in entropy, ΔE is the change in energy, ρ is the density and Δs_{1-2} is the change in specific entropy. Njoku et al. [11] used a entropy generation number defined as

$$N_s = \frac{\dot{S}_{gen}(t)}{\dot{S}_{gen,max}(t)}, \qquad (26)$$

where $\dot{S}_{gen}$ is the entropy generation and $\dot{S}_{gen,max}$ is the maximum entropy generation in the tank. The entropy generation is defined as $\dot{S}_{gen} = \sum_{i=1}^{N} \dot{S}'''_{gen} V_i$, where $\dot{S}'''_{gen}$ is the volumetric entropy generation rate. In cylindrical coordinates this is expressed as

$$\dot{S}'''_{gen} = \frac{k}{T^2}\left[\left(\frac{\partial T}{\partial r}\right)^2 + \left(\frac{\partial T}{\partial z}\right)^2\right] + \frac{\mu}{T}\left[2\left\{\left(\frac{\partial v_r}{\partial r}\right)^2 + \left(\frac{v_r}{r}\right)^2 + \left(\frac{\partial v_z}{\partial z}\right)^2\right\} + \left(\frac{\partial v_z}{\partial r} + \frac{\partial v_r}{\partial z}\right)^2\right],$$
$$(27)$$

where r is the radial distance and z is the axial distance. This entropy generation number was compared to an energy efficiency (ratio of energy flow into the tank to the energy accumulation in the tank) and an normalized exergy efficiency (compares exergy in the tank to exergy in ideally stratified and fully-mixed tank), and it was found that the entropy generation number was better able to represent the stratification. Njoku et al has continued examining the entropy generation numbers in later studies [3]. This method is similar to the one developed by Hunh [34]. Hunh used the same entropy generation number as Njoku et al. but reversed the scale, $N_{s,hunh} = 1 - N_{s,Njoku}$.

Comparative studies of these and other methods have been done by Haller et al. [35] and Castell et al. [36] among others. Castell only looked at different dimensionless numbers and found that the Richardson number was the dimensionless number that best represented stratification, but it was only able to qualify not quantify stratification. Haller et al. compared different methods and compared them to the rate of entropy production due to mixing, a summation of the results found can be seen in table 1.

The two first methods mentioned in the table is not part of this study. The MIX_{And} is the same MIX number as developed by Davidson et al. but using different methods to calculate

the moment of energy. The method used by Panthalookaran et al. was also investigated but is not part of the table since it was recently developed when Haller et al. published. As with the MIX number, Panthalookaran et al. were also able to isolate heat loss from mixing. For charging and discharge the method of Hunh was found to best represent the stratification of the tank, for storing Hunh and Panthalookaran et al. returned the same results.

Table 1 – General characteristics of selected indices for the degree of stratification and stratification efficiency definitions for TES processes [35, Table 1].

	Index for degree of stratification	Stratification efficiency or ratio	Applicable for charging	Applicable for discharging	Applicable for storing/ standby	Identification of the instant of destratification or mixing possible	Isolate mixing from heat losses	Applicable to variable temperatures and mass flows	In qualitative agreement with entropy production	Internal temperature measurement needed
Thermocline thickness and related methods	X	0	X	X	X	X	0	0	–	O/X
Wu & Bannerot (1987)	X	0	X	X	X	X	0	?	–	X
Discharge/charge efficiences	0	X	X	X	0	0	0	0	0	0/X
MIX_{Dav}, Davidson et al. (1994)	0	X	X	0	X	X	X	(X)	0	X
MIX_{And}, Anderson et al. (2007)	0	X	X	X	X	X	X	(X)	0	X
Shah & Furbo (2003)	0	X	X	X	X	X	0	0	0	X
Huhn (2007) / van Berkel (1997)	0	X	X	X	X	X	0	X	X	X

X, applies for this method; 0, does not apply for this method; (X), limited application; ?, unknown.

3 Method

3.1 The experimental tank

An experimental tank has been used during this project to base the CFD model on. The tank is an EWHT from CTC. It is a regular water heater for private households with some modifications. The tank has been mounted with three temperature sensors at different heights in the tank, to measure the temperature in the tank. These temperature sensors measure the temperature in the middle of the tank, at their respective heights. Temperature sensors have also been mounted on the inlet and outlet of the tank, and a valve has been fitted to the outlet. This is all illustrated in figure 5. A relay has been mounted to the heating element to manually control when the tank turns on the heating element. National Instrument DAQs have been used both to control the heating element and valve in addition to reading data from the temperature sensors. To control this, a LabView program has been set up to control the different parameters. The power used by the heating element is measured with a power relay from E2U. This system was built in collaboration with Marius Christoffersen as part of his master thesis[37] and is explained in more detail in Appendix A.

3.2 Building the model in COMSOL

The program used for the CFD model in COMSOL. In this section, an explanation of building and verifying the model has been given. Firstly the geometry of the model should be defined. There is some uncertainty about how the geometry inside the tank is built up and inquires to the producer has not yielded satisfactory explanations. The only information available about the geometry inside the tank is shown in figure 4. No measurements or the exact geometry of the inlet has been found. The building of model must then be done by using experimental results to verify the geometry used inside the tank. When building the geometry, there is possible to import a 3D model from CAD software and use this for the simulation. Using a 3D model gives a more exact model especially when simulating complex 3D geometries. In this case, the main geometry is a cylinder, an axisymmetrical shape, and a 2D axisymmetrical model will be presented. The 2D axisymmetrical model works by modeling a cross-section of the geometry, and when modeling, COMSOL will revolve around the cross-section about an axis. In this type of modeling there is not a θ axis, and only a r and z axis, so for a given r and z the value has to be the same for all values of θ. By using this method, it is possible to reduce the computational time by only introducing one restriction on the model, namely that all parts of it need to be axisymmetrical. Care has to be given when using such a model since the heat and flow may not be axisymmetric even if the geometry is.

The geometry supplied by the manufacturer states that the tank has an outside height of 1.14 m and a water volume of 194 liters. The other dimensions are found by manual measurements and calculations. The inlet, outlet, and heating element must be placed differently from the real tank to comply with axisymmetry. The inlet has been placed in the middle of the tank coming in from the bottom wall and releasing the water to the side through a perforated plate to simulate the diffuser used in the tank. The outlet is modeled in the top of the tank accepting water vertically. The heating element is modeled as a disk in the middle of the tank. An air domain has also been modeled around the tank to enable heat transfer to the environment.
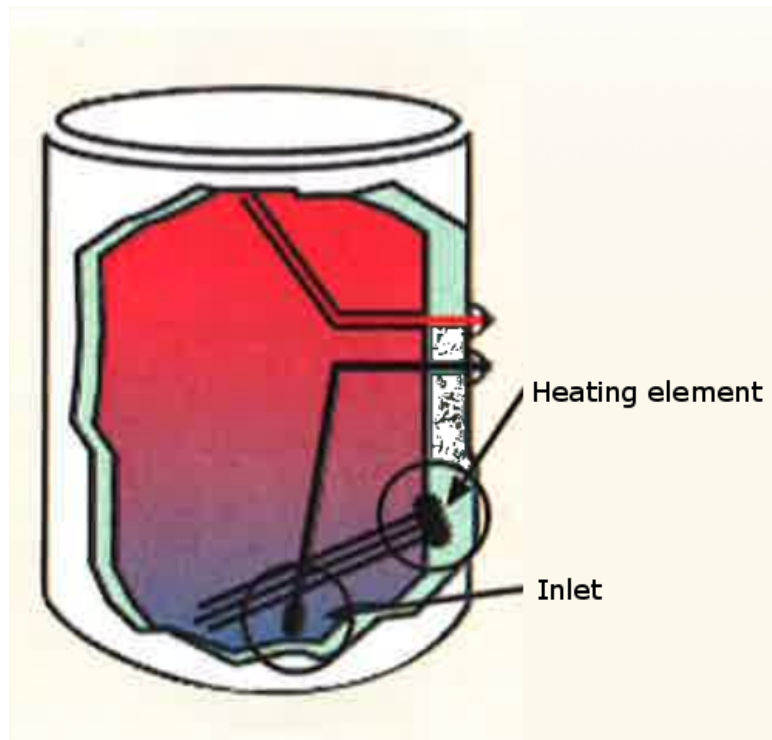
UNIVERSITY OF AGDER

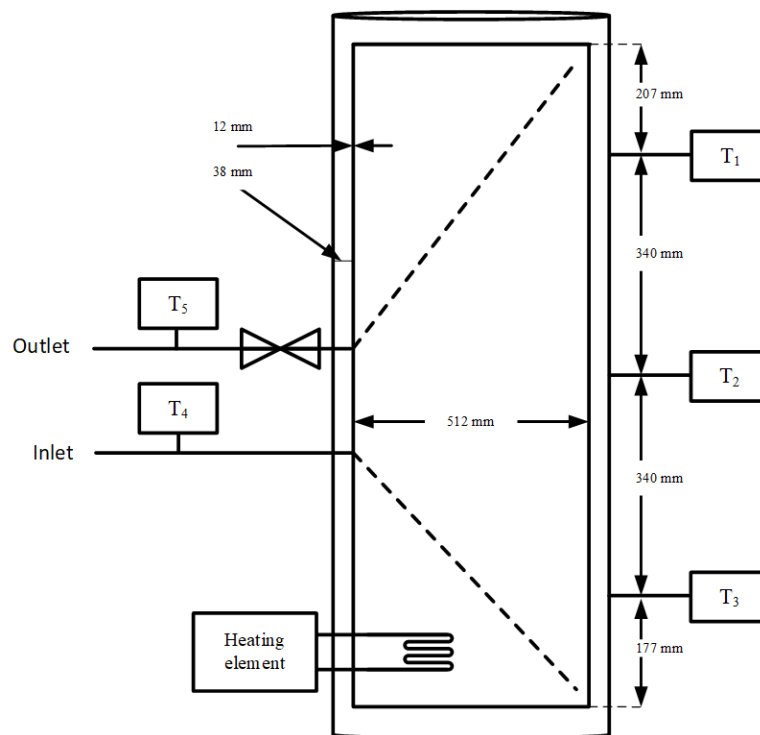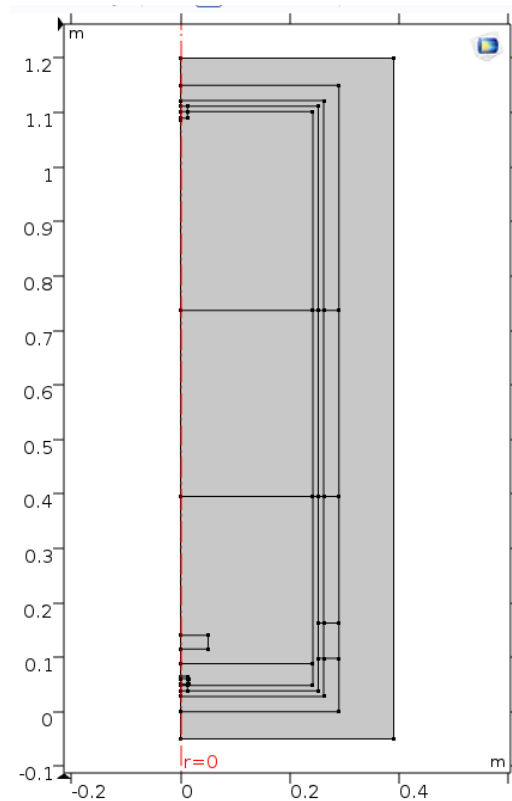**Figure 4** – Diagram of EWHT from CTC

Figure 5 – Dimensions of tank

The geometry built can be seen in figure 6.

Figure 6 – The tank geometry as modelled in COMSOL

To model the physics of the tank, a multiphysics model for isothermal flow has been used. This model connects the physics of the flow and heat transfer physics in COMSOL. For the flow model, a laminar flow has been chosen. When the tank is either heating or cooling down, and no flow is coming through the inlet, the flow will be laminar. This can be shown by calculating the Rayleigh number for the surfaces in the tank with the natural flow the flow transitions from laminar flow to turbulent when $Ra > 10^8$. If eq 12 is solved for ΔT then the temperature difference will have to be in the range of $\Delta T > 10^5$ for $Ra = 10^8$ so the flow here will be laminar.

For the case where the inlet is open, it must be assumed that there is some turbulence as water enters the tank. However, the model was tested with a laminar flow model for this regime too and gave good results, so a laminar model was chosen to save on computational cost in addition to making it easier to simulate a flow regime, followed by a heat loss or heating regime in the same model.

After choosing the physics of the system, the boundary conditions must be set up for each of the two physics models.

For the laminar flow:

Wall   Defines the walls around the fluids, using a 'no-slip' boundary.

Open Boundary Allows a free flow into and out of the air domain.

Inlet Inlet placed in the bottom of the tank, and the flow is defined with velocity.

Outlet Placed in the top of the tank and defined with pressure.

Screen Boundary in front of the inlet defined as a perforated plate with a solidity of 0.9 to simulate the diffuser on the inlet in the real tank

For heat transfer in fluids:

Open Boundary Allows flow of heat into and out of the air domain from an environment with ambient temperature.

Temperature Defines a temperature on the inlet to set the temperature of the water flowing into the tank.

Heat Source Defines the heating element in the tank.

The model has been meshed with a physics defined mesh in COMSOL, and this means that it uses a mesh generation pre-defined by COMSOL based on the different physics and boundary conditions used in the model. COMSOL has seven different pre-defined sizes for mesh elements from 'extremely coarse' to 'extremely fine'. For this model, the normal size is chosen. With these parameters, COMSOL then chooses a size for the different domains based on the model. For the fluids, it chooses a coarse size, for solids it chooses the normal size and for the transitions between solids and fluids it is sized to fine. All of these meshes uses thetrahedrals. Near the wall, a boundary layer mesh is applied. These are two layers of quadrilaterals with have a large height to width ratio to deal with the convective flow that will occur along the walls. The meshed model is shown in figure 7

3.3 Validating the model

To validate the model built in COMSOL, it is compared to data from an experimental tank. In COMSOL the temperature is probed at the same heights as the temperature sensors in the experimental tank. The inlet temperature measured at the inlet has been used for the inlet temperature in COMSOL when comparing discharge. For the heating element, the energy used has been measured with a power relay, and this is the value used for the heat source in COMSOL. In addition to the three probes used to validate the model 9 points equidistant from each other throughout the height of the tank is used to get a better idea of the temperature difference throughout the tank. The temperature has also been measured right below the outlet to see the temperature of the water leaving the tank.
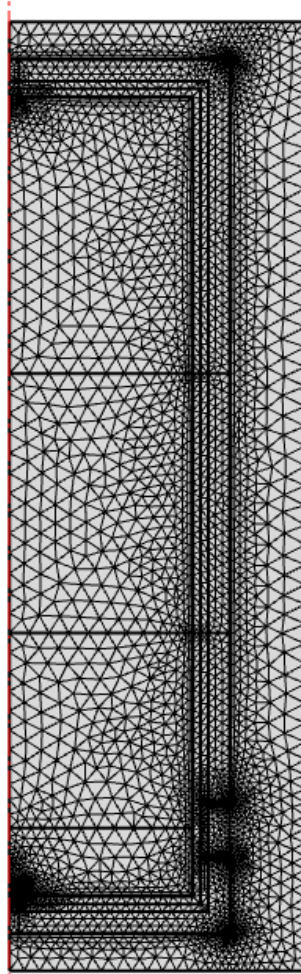
Figure 7 – Meshed model

The experiments used to validate the model is:

Full discharge   In this experiment the water flows into the tank and continue until the tank has a uniform temperature equal to the inlet temp.

Heating + Cool-down Here the water in the tank is first heated before the heating element is turned off and the tank starts a cool-down period.

Cool-down   For the cool-down experiment the tank starts at a given temperature and with no heating or inflow as the tank cools-down.

3.4 Stratification efficiency from different inflow rates

When the physical system was assembled the water flow was measured from the tank, and it was found to be around $0.36kg/s$. This was found by opening the valve of the tank and measuring the amount of water coming out of the tank. This was done multiple times, and Labview was used to control the valve to get consistent closing times. The value of $0.36kg/s$

was then found by taking the average of these experiments. The results of these experiments are shown in Appendix B. The COMSOL model has been used to investigate how different values for the inflow rate will affect stratification. The method used for this is the entropy generation number of Njoku et al. (N_s)[11].

Seven different flow regimes have been chosen every other boundary in the model has been kept constant between the experiments. The flow regimes chosen are: $0.15kg/s$, $0.20kg/s$, $0.25kg/s$, $0.30kg/s$, $0.36kg/s$, $0.40kg/s$ and $0.50kg/s$. All experiments have been started with the initial temperature of the tank at $70°C$ in the whole tank, and the temperature of the water flowing into the tank is set to $10°C$ and is constant throughout the simulation. All simulations are run for 1200 seconds.

The entropy generation ($\dot{S}_{gen}$) from equation 27 has been calculated in COMSOL using integration coupling. The maximum entropy generation ($\dot{S}_{gen,max}$) will occur when the tank is fully mixed and can be calculated as,

$$\dot{S}_{gen,max} = \dot{m}c_p \left[\frac{(T_{in} - T_{ini})exp(-\varphi)}{T_{in} - (T_{in} - T_{ini})exp(-\varphi)} - ln\left(\frac{T_{in}}{T_{in} - (T_{ini}exp(-\varphi))} \right) \right] , \qquad (28)$$

where φ is the fraction of the storage volume that has been replaced with the cold water from the inlet and is given by,

$$\varphi = \frac{A_{in}Ut}{V} , \qquad (29)$$

where A_{in} is the area of the inlet and t is the time from the valve opened.

It is then possible to compare the entropy generation in the tank with the theoretical maximum entropy generation possible as,

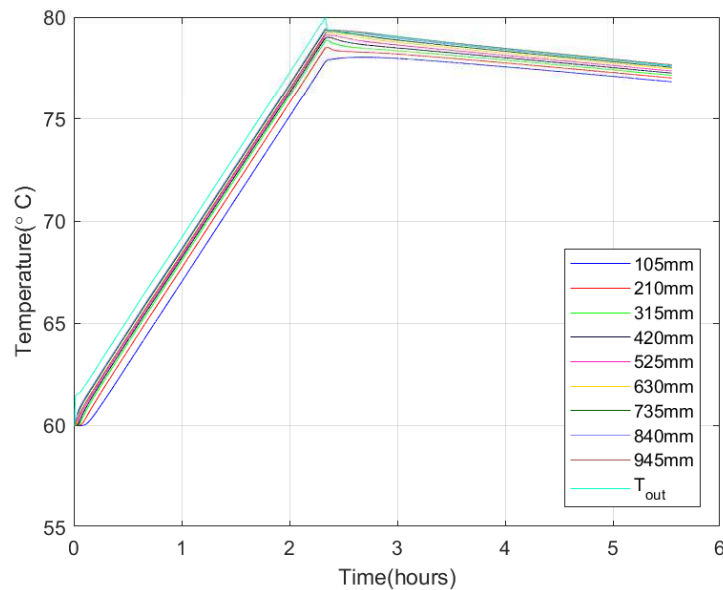$$N_s = \frac{\dot{S}_{gen}}{\dot{S}_{gen,max}} , \qquad (30)$$

and here 0 represents an ideally stratified tank while 1 represents a fully mixed tank.

The entropy generation number has been calculated for each timestep and plotted to illustrate the change during different discharges.

4 Results
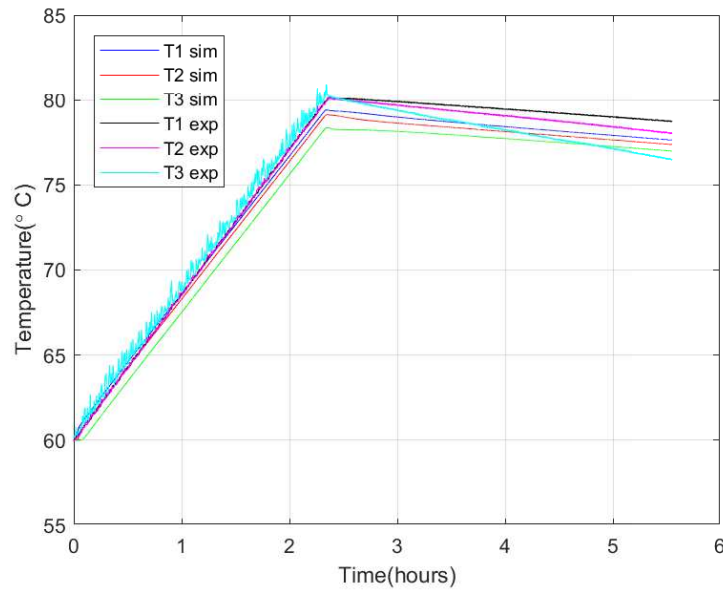
(a) Compared with experimental results

(b) With 9 temperature sensors placed equadistance in the tank

Figure 8 – Heating and Cool-down

From figure 8a an experiment with heating from $60 - 80°C$, followed by a cool-down period of about 4 hours. During the heating part of the simulations, the top and middle temperatures follow the experimental results very good, but the simulations have a pronounced stratification during heating that is not found during the experiments. The simulation ends the heating part of the experiments with a slightly lower temperature than what the experimental results show. During the cool-down phase of the simulations the stratification that have developed

while heating shrinks. However, for the experimental tank where there was no stratification during heating, and stratification only occurs when the heating element is turned off.

When looking at the figure with more temperature sensors(figure 8b) it can be seen that the stratification gets more pronounced near the bottom of the tank as well as near the very top. In the middle of the tank, there are only small differences in temperature. In figure 10 there is possible to see some interesting observations about the temperature distribution during heating. While the temperature near the outlet (T_{out}) is the highest temperature in the tank, the temperature sensor right below $945mm$ is not the second highest temperature. While it seems the temperature in the tank is distributed with a higher temperature the further up in the tank the measurement is taken. Near the very top where $T9$ is placed the temperature is equal to $630mm$ and lower than the two temperature sensors in-between ($735mm$ and $840mm$). In figure 9a The flow induced from the heating element is illustrated. The nine equidistant temperature sensors are placed out to the right in the model, this may be some of the explanation for the temperature distribution in the top of the tank, as the flow goes around the area where $945mm$ is placed and ends in the area of $840mm$ and $735mm$. The flow seen on the outside of the tank is the convective flow due to the temperature difference between the tank and the ambient air. This flow is present during the whole simulation.


(a) During Heating

(b) During discharge
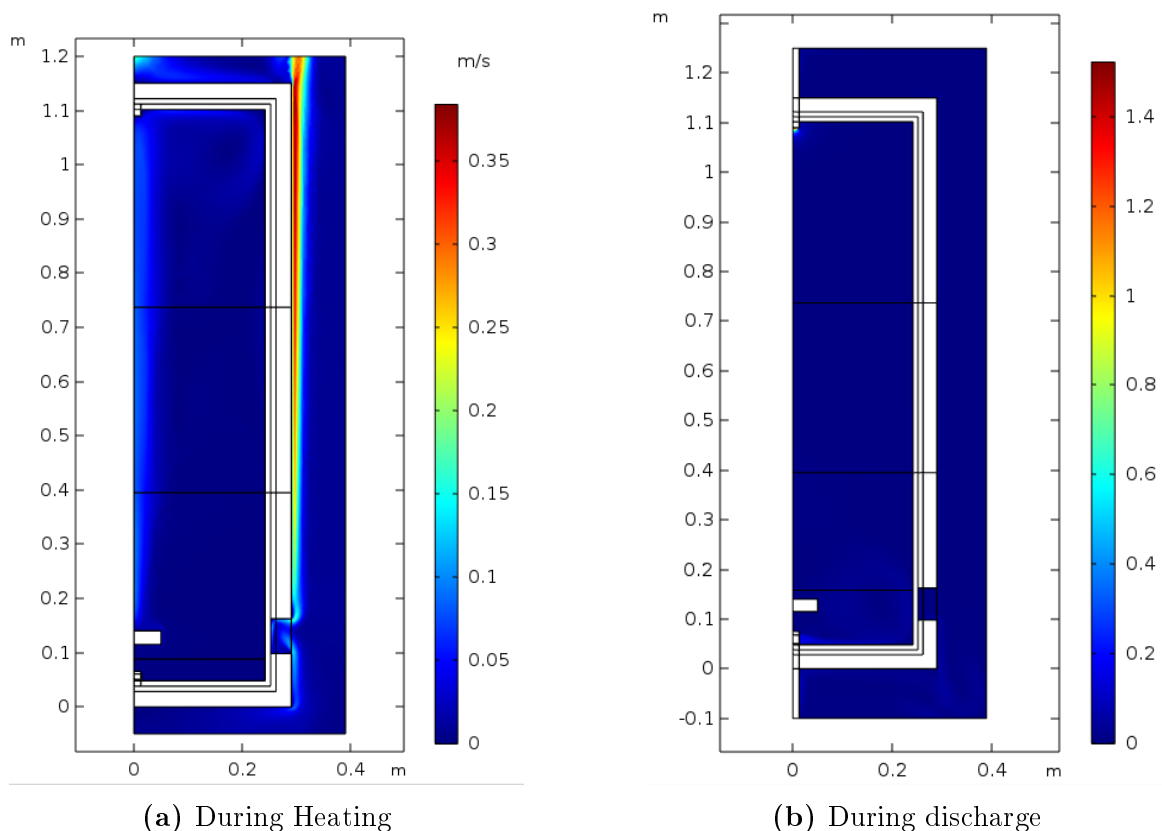
Figure 9 – Flow in the tank

22
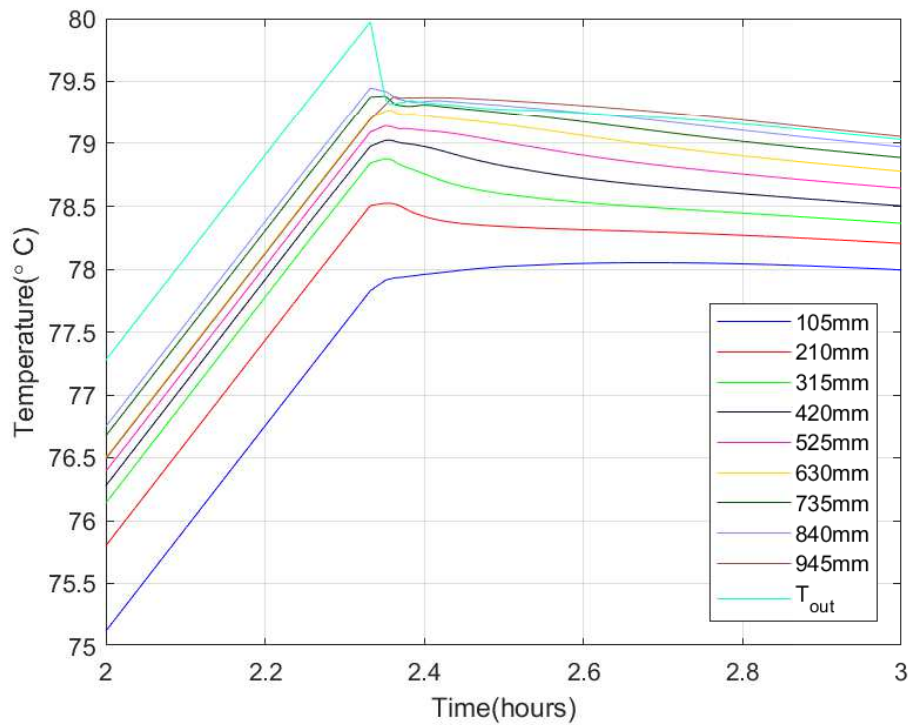
Figure 10 – View of the transition between heating and cool-down

In figure 11a the experiments from a cool-down test have been compared with experimental results. In the top of the tank, it can be seen that the data from the simulations correspond to the data from the experiments, but lower in the tank, the temperature is not falling as rapidly as in the real tank. When looking at the 9 equidistant temperature sensors (figure 11b) Firstly, it should be noted that since the experiment started with some stratification, and the tank only has three temperature sensors, the tank was split into three parts when setting initial values for the simulation. Between the temperature sensors in the real tank, there is also stratification but it is unknown. For this reason, three and three of the heights start out at the same temperature before moving in separate directions as the tank moves toward a similar stratification as was seen in figure 8. The outlet temperature falls significantly during the beginning of the simulation before rising again and settling near the temperature in the middle of the tank. This is most likely because of some flow occurring near the outlet, but because of the convective flow on the outside of the tank being relatively high(similar to the convective flow in figure 9a) there are no visible flows inside the tank during this experiment.
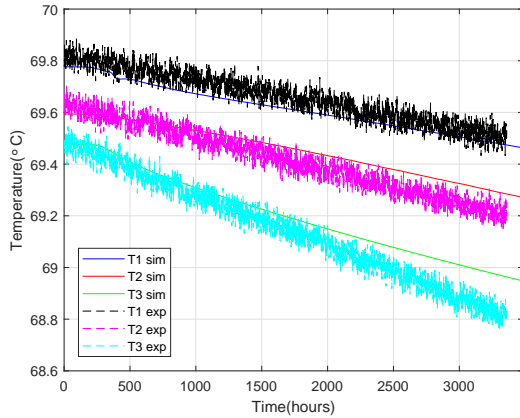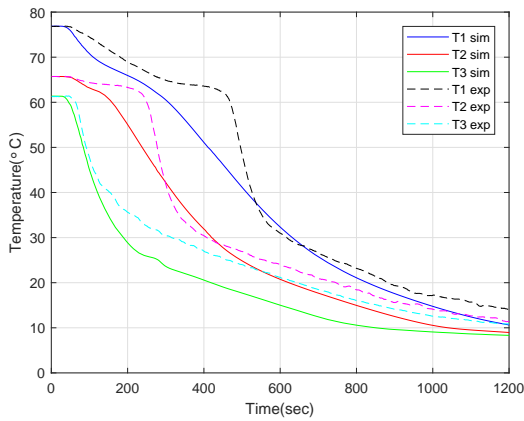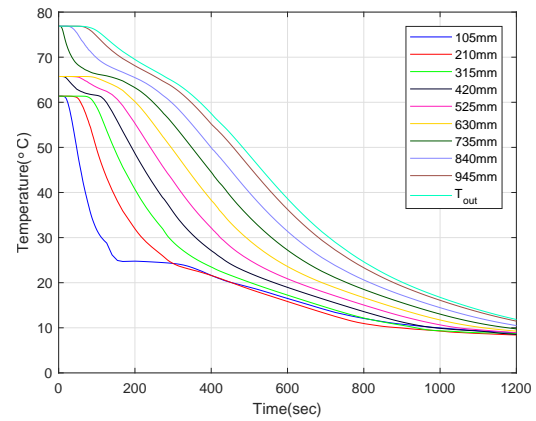
(a) Compared with experimental results
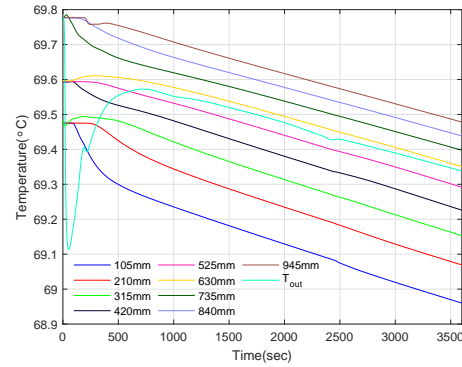
(b) With 9 temperature sensors placed equadistance in the tank

Figure 11 – Heat loss over one hour

(a) Compared with experimental results

(b) With 9 temperature sensors placed equadistance in the tank

Figure 12 – Full discharge of the tank

For the discharge experiment (figure 12) it can be seen in the experiment that the temperatures near the top of the tank start falling earlier than in the experimental tank. The temperatures in the top and middle of the tank start falling faster than what is the case for the experimental tank. The final temperature is also lower than what is the case for the real tank. After 20 minutes all the temperatures in the simulated tank is below the lowest temperature from the experiments. The curves do have a similar shape in both simulation and experiment although the experiments have sharper corners when the temperature starts falling. When looking at nine temperature sensors in the tank, it can be observed that in the bottom of the tank the temperatures do not fall all the way down to around 10 degrees before they converge. The lowest temperature sensor ($105mm$) only falls to $25°C$ before leveling off and continues to fall only when the temperature over a larger volume reaches the same temperature. In the rest of the tank, the temperatures are falling at a similar rate. In figure 9b the flow in the tank during discharge can be seen. The water comes into the tank horizontally and flows upwards in the tank as it hits the wall.

(a) The first 50 seconds

(b) 1200 seconds
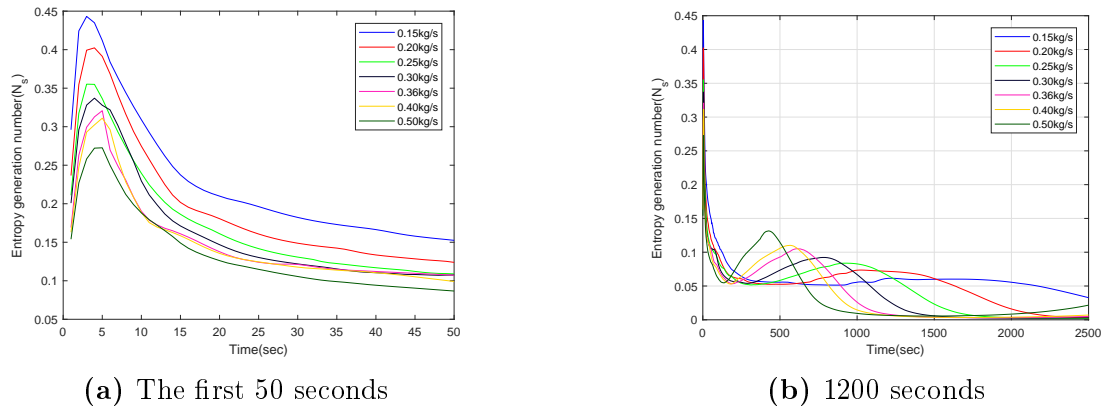
Figure 13 – Entropy generation number

4.1 Entropy Generation Number

In figure 14 the temperatures is shown for the simulations with different inlet flow rate is shown. As would be assumed, for larger mass flow rates the temperature starts dropping faster. The leveling off in the bottom of the tank is not as pronounced or happening as early when the tank starts at a uniform temperature. It is only noticeable here for the two largest discharges. Until the water in the outlet reaches $40°C$ the water is usable as hot water. The energy extracted from the tank before the outlet temperature reaches $40°C$ is shown in table 2, the table also shows the amount of water at the initial temperature that can be extracted from the tank. From the smallest discharge to the largest it is possible to extract $3MJ$ more from the tank as usable hot water, and the amount of energy always rises for higher discharge. For water at initial temperature, the highest amount is when the discharge is $0.40kg/s$.

Table 2 – Energy extracted while the temperature in the tank is above $40°C$

Mass flow	0.15kg/s	0.20kg/s	0.25kg/s	0.30kg/s	0.36kg/s	0.40kg/s	0.50kg/s
Energy	41.35MJ	42.57MJ	42.96MJ	43.72MJ	44.34MJ	44.56MJ	44.87MJ
Kg water at 70°C	63kg	69.4kg	76.75kg	85.8kg	90.72kg	94kg	91.5kg

For the entropy generation number, the form of the curves are similar, it starts high and starts falling before getting a small jump after the initial fall before they stabilize around the same point. During the first 5 seconds, the entropy generation is rising implying a tank that gets more and more mixed, although the tank starts at a uniform temperature and is therefore never as fully mixed as at the beginning of the experiment. After the first 5 seconds, all discharges reaches its highest entropy generation number. The lowest discharges reach the highest entropy generation numbers suggesting a better stratified tank for the higher discharges. This remains true for the beginning of the experiments until the values for the higher discharges start rising again. Before the rise, all discharges converge around an entropy generation number of 0.05, after the rise all values converge even lower around 0.01. Towards the end of the simulation, it can be seen that the larges discharge ($0.5kg/s$) starts rising again, but from the temperatures for this discharge (figure 14g) the temperatures are the same as they have been for the last 1800 seconds.
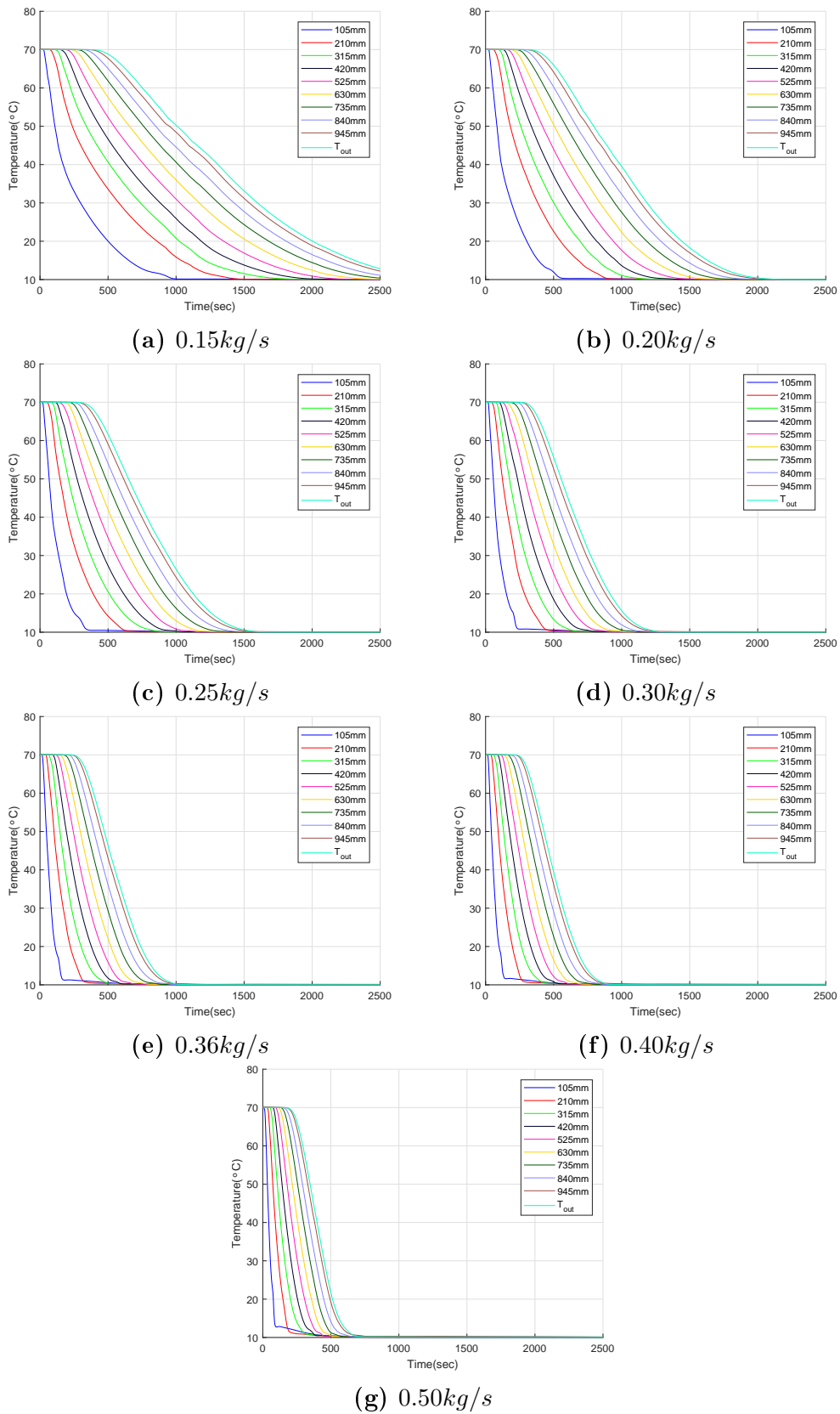
(a) $0.15 kg/s$

(b) $0.20 kg/s$

(c) $0.25 kg/s$

(d) $0.30 kg/s$

(e) $0.36 kg/s$

(f) $0.40 kg/s$

(g) $0.50 kg/s$

Figure 14 – Temperatures in the tank for the different mass flow regimes

26

5 Discussion

From the results, it can be seen that the simulations return similar results as the experimental data obtained in the real tank. In the heat loss experiments, the heat loss in the top of the tank corresponds well to the experiments while in the bottom the loss in the real tank is higher than in the experiments. There must be some heat loss in the tank that is not accounted for in the model. In the bottom of the tank there where the heating element is connected, there is a volume that is not isolated with glass wool as the rest of the tank. Since the tank is very well insulated, this means that the unisolated part of the tank has a relatively high loss compared to the rest of the tank. This unisolated area has been modeled into COMSOL, and it would be assumed since the model still not corresponds fully that there are some other areas of the tank that is similarly not isolated, but more information about the tank is needed to draw any conclusions about this.

For the discharge simulations, no flowmeter has been mounted on the tank, and although the flow rate was measured. It is not necessarily right for each experiment. The flow rate into the tank will be affected by the water usage in the rest of the building. The pressure in the water lines will change depending on how much water is being used throughout the building. This will create a variable that is not possible to adequately account for when running the simulations, without real-time data of the flow during the experiments.

During the heating experiments, there are some temperature differences in the simulation that is not present in the real tank. In figure 9a it can be seen that most of the flow due to the heating element happens in the middle of the tank. It may be the case that the flow is more distributed in the real tank, making the temperatures throughout the tank more equal. In the real tank, the temperatures are measured in the middle of the tank for each height. If the same is done in the simulation during heating, the temperature difference at different heights gets even more pronounced with the highest temperatures lowest in the tank, nearer the heating element. The heating element in the COMSOL model is different from the element in the real tank. In the real tank, the heating element is a cylinder mounted on one side of the tank and angled slightly downward. While in the model it is a round disc placed in the middle of the tank, near the bottom.

From table 2 it can be seen that if the goal is to extract as much energy as possible from the tank, a higher discharge is better. It would have to be assumed that this would not be the case if the mass flow rate into the tank were raised even more. It can already be seen that the higher inflow rate gives diminishing returns. Between the the two lowest discharges ($0.15kg/s$ and $0.20kg/s$) there is a difference of over $1MJ$, but for the two largest discharges $0.40kg/s$ and $0.50kg/s$ the difference is only $300KJ$. At some point raising the mass flow rate would give lower values again. This can already be seen in the amount possible to extract at the initial value of the tank. The highest value here does not give the most hot water at initial temperatures, but rather the discharge of $0.40kg/s$ does.

From the temperature distribution in the multiple discharge experiments, the higher discharges get steeper curves and start to fall faster. If comparing $0.50kg/s$ and $0.25kg/s$, for the $0.50kg/s$ experiment the outlet temperature starts falling after 200 seconds and for the $0.25kg/s$ experiment the outlet temperature starts falling after 375 seconds. This means that for the larger

discharge there is possible to extract more water at the initial temperature than for the lower discharge case as table 2 shows. When the outlet temperature reaches $40°C$, it takes double the time to reach with half the discharge. This seems to be true for all heights and discharges. So for larger discharges, it is possible to extract more hot water.

For the entropy generation number at the beginning, the lowest flow rates start less stratified than the higher flow rates. This is because at the beginning more of the tank is still at initial values for the lower flow rates. With higher flow rates the entropy generation number is better during the first 200 seconds before they either all converge around 0.05 or starts rising again as the bottom of the tank reaches the inlet temperature. All the graphs start rising again after a while but at different times, with the highest flow rate rising first. This happens as the lower part of the tank reach the inflow temperature. However, starts sinking again as most of the tank reaches the lowest flow rate. This would suggest that while the entropy generation number might be a good way to compare the stratification between experiments as suggested by Haller et al.[35] it does not produce good results towards the end of a full discharge. In all the experiments the entropy generation number starts sinking, suggesting better stratification, around the time the height of $630mm$ reaches the inflow temperature. It would be expected that the entropy generation number would get lower as the temperature difference gets more prominent, and most of the layers have a temperature between the initial and inflow temperature. While it should start rising again as more of the layers reach the inflow temperature and then continue rising towards 1 as the tank becomes mixed again at the inlet temperature.

In section 2.4.1 a few design suggestions from the literature has been discussed. The difference between these suggestions and the real EWHT used in these experiments could suggest improvements to make the stratification in the tank better.

The first design parameter discussed in the literature was the H/D ratio, that Lavan and Thompson[22] that suggested a ratio between 3 and 4, this was later confirmed by other research[23–25]. The experimental tank used in this paper has an inner height of $1.064m$ and diameter of $0.512m$ giving an H/D ratio of 2. This would suggest there are possible to improve the stratification with a higher H/D ratio. For a $194l$ tank with H/D ratio of 4 would have a height of approximately $1.58m$ and diameter of $0.4m$.

Yang et al.[21] suggested that a cylinder is the worst geometry both for stratification and energy storage capacity. Compared to stratification, the shapes that gave the best results was shapes with sharp corners. These are not shapes that are easy to place standing and would be in need of struts to balance vertically. For the shapes that gave better exergy and energy capacity such as a barrel, these are not as volume effective as a cylinder.

For the tank inlets and obstacles inside the tank, the tank is fitted with a diffuser as gave some positive results in the study done by Moncho-Esteve et al[12]. There are no obstacles placed in the tank, but looking at figure 9b it could help by containing the flow lower in the tank than what is the case at this point.

Although there is possible to use this CFD model to simulate discharge, heating, and cooldown, it is at the moment not possible to simulate all three regimes in the same simulation.

When adding all the boundary layers to the model, e.g., the temperature boundary layer is only needed when simulating discharge and is not used when simulating the other regimes. When adding both the temperature and screen boundary while not simulating discharge, the simulation will not converge, and it is not possible to model heating or cool-down with both of these boundaries added. There is therefore not possible at the moment to simulate a real use of the tank. The problem with adding these two boundaries without any mass flow into the tank is that the temperature difference between the water in the tank and the temperature on the boundary creates some small flows through the screen that COMSOL cannot calculate. There has also been tried to turn one or both of these boundaries off and turn them on when coming to the discharge part of the experiment but this has not given any results either.

6 Conclusion

In this thesis, a CFD model of an EWHT has been built and used to simulate the tank. The CFD model has been validated against experimental results from a real EWHT. The model has been used to test the effect on the tank with different flow rates. It was found for larger flow rates that the tank was able to deliver more useful hot water than at lower flow rates. It was also found that the returns started to diminish and it would be assumed that at some point a higher flow rate would be worse for the tank. Calculations of an entropy generation number to compare the stratification in the tank at the different flow rates also showed a better stratification for a higher flow rate.

The experimental tank has been compared to design parameters given in the literature to improve the stratification in the tank. It was found that there could be possible to improve the stratification by raising the H/D ratio and mounting some obstacles near the bottom of the tank. Although these parameters have been discussed these different designs have not been simulated in this study.

The validation of the model gave some good results, but there are still differences in the results from the simulations and the experimental data. While a model has been built that can simulate all the operations of the EWHT, the model is still unable to connect all the different operations in a single study to simulate the real operations of the tank over time.

7 Further Work

In this section suggestions for further work on the system used in this paper is presented. Firstly the model should be developed further to be able to simulate the real operations of the tank over different operations. Further work could also study the different design parameters such as the H/D ratio and its effect on stratification on this tank.

If the tank should be controlled to act as a battery for a PV system, a grey box or analytical model should be developed from the simulated data to be able to predict the outlet temperature of the tank, with measurements obtainable from outside the tank, such as flow or inlet temperature.

Bibliography

[1] A. R. Hval, "Stratification in electric water heater", 2017.

[2] O. Dumont, C. Carmo, R. Dickes, E. Georges, S. Quoilin, and V. Lemort, "Hot water tanks: How to select the optimal modelling approach?", in *CLIMA 2016-12th REHVA World Congress, 22-25 May 2016, Aalborg, Denmark*, Aalborg University: Department of Civil Engineering, 2016.

[3] H. O. Njoku, O. V. Ekechukwu, and S. O. Onyegegbu, "Numerical investigation of entropy generation in stratified thermal stores", *Journal of Energy Resources Technology*, vol. 140, no. 1, p. 011 901, 2018.

[4] Y. H. Zurigat, K. J. Maloney, and A. J. Ghajar, "A comparison study of one-dimensional models for stratified thermal storage tanks", *Journal of Solar Energy Engineering*, vol. 111, no. 3, pp. 204–210, 1989.

[5] R. Dickes, A. Desideri, V. Lemort, and S. Quoilin, "Model reduction for simulating the dynamic behavior of parabolic troughs and a thermocline energy storage in a micro-solar power unit", *Proceedings of ECOS 2015*, 2015.

[6] D. E. Adams and J. H. Davidson, "Tank stratification with a flexible manifold", in *The 1993 American Solar Energy Society Annual Conference, American Solar Energy Society, Washington, DC*, 1993.

[7] N. K. Ghaddar and A. M. Al-Maarafie, "Study of charging of stratified storage tanks with finite wall thickness", *International journal of energy research*, vol. 21, no. 5, pp. 411–427, 1997.

[8] J. H. Davidson, D. A. Adams, and J. A. Miller, "A coefficient to characterize mixing in solar water storage tanks", *Journal of Solar Energy Engineering*, vol. 116, no. 2, pp. 94–99, 1994.

[9] B. J. Newton, "Modeling of solar storage tanks", Master's thesis, University of Wisconsin–Madison, 1995.

[10] C. A. Cruickshank and S. J. Harrison, "Heat loss characteristics for a typical solar domestic hot water storage", *Energy and buildings*, vol. 42, no. 10, pp. 1703–1710, 2010.

[11] H. O. Njoku, O. V. Ekechukwu, and S. O. Onyegegbu, "Comparison of energy, exergy and entropy generation-based criteria for evaluating stratified thermal store performances", *Energy and Buildings*, vol. 124, pp. 141–152, 2016.

[12] I. J. Moncho-Esteve, M. Gasque, P. González-Altozano, and G. Palau-Salvador, "Simple inlet devices and their influence on thermal stratification in a hot water storage tank.", *Energy and Buildings*, vol. 150, pp. 625–638, 2017.

[13] L. Kong, W. Yuan, and N. Zhu, "Cfd simulations of thermal stratification heat storage water tank with an inside cylinder with openings", *Procedia Engineering*, vol. 146, pp. 394–399, 2016.

[14] Z. Wang, H. Zhang, B. Dou, H. Huang, W. Wu, and Z. Wang, "Experimental and numerical research of thermal stratification with a novel inlet in a dynamic hot water storage tank", *Renewable Energy*, vol. 111, pp. 353–371, 2017.

[15] H. K. Versteeg and W. Malalasekera, "Implementation of boundary conditions", in *An introduction to computational fluid dynamics: the finite volume method*, 2nd ed. Pearson Education, 2007, pp. 267–284.

[16] V. D. Liseikin, in *Grid generation methods*, 3rd ed. Springer, 1999, vol. 1, p. 3.

[17] C. Cristofari, G. Notton, P. Poggi, and A. Louche, "Influence of the flow rate and the tank stratification degree on the performances of a solar flat-plate collector", *International Journal of Thermal Sciences*, vol. 42, no. 5, pp. 455–469, 2003.

[18] E. M. Kindle, "A comparative study of different types of thermal stratification in lakes and their influence on the formation of marl", *The Journal of Geology*, vol. 37, no. 2, pp. 150–157, 1929.

[19] S. Yoshimura, "A contribution to the knowledge of deep water temperatures of japanese lakes", *Japanese Journal of Astronomy and Geophysics*, vol. 13, p. 61, 1935.

[20] J. van Berkel, C. C. M. Rindt, and A. A. van Steenhoven, "Modelling of two-layer stratified stores", *Solar Energy*, vol. 67, no. 1, pp. 65–78, 1999.

[21] Z. Yang, H. Chen, L. Wang, Y. Sheng, and Y. Wang, "Comparative study of the influences of different water tank shapes on thermal energy storage capacity and thermal stratification", *Renewable Energy*, vol. 85, pp. 31–44, 2016.

[22] Z. Lavan and J. Thompson, "Experimental study of thermally stratified hot water storage tanks", *Solar Energy*, vol. 19, no. 5, pp. 519–524, 1977.

[23] A. J. N. Khalifa, A. T. Mustafa, and F. A. Khammas, "Experimental study of temperature stratification in a thermal storage tank in the static mode for different aspect ratios", *ARPN journal of Engineering and Applied Sciences*, vol. 6, no. 2, pp. 53–60, 2011.

[24] K. A. R. Ismail, J. F. B. Leal, and M. A. Zanardi, "Models of liquid storage tanks", *Energy*, vol. 22, no. 8, pp. 805–815, 1997.

[25] E. Hahne and Y. Chen, "Numerical study of flow and heat transfer characteristics in hot water stores", *Solar Energy*, vol. 64, no. 1, pp. 9–18, 1998.

[26] Y. H. Zurigat, A. J. Ghajar, and P. M. Moretti, "Stratified thermal storage tank inlet mixing characterization", *Applied Energy*, vol. 30, no. 2, pp. 99–111, 1988.

[27] A. Bouhdjar, A. Benkhelifa, and A. Harhad, "Numerical study of transient mixed convection in a cylindrical cavity", *Numerical Heat Transfer, Part A Applications*, vol. 31, no. 3, pp. 305–324, 1997.

[28] N. Altuntop, M. Arslan, V. Ozceyhan, and M. Kanoglu, "Effect of obstacles on thermal stratification in hot water storage tanks", *Applied thermal engineering*, vol. 25, no. 14, pp. 2285–2298, 2005.

[29] A. Aviv, Y. Blyakhman, O. Beeri, G. Ziskind, and R. Letan, "Experimental and numerical study of mixing in a hot-water storage tank", *Journal of Solar Energy Engineering*, vol. 131, no. 1, p. 011011, 2009.

[30] M. A. Rosen, R. Tang, and I. Dincer, "Effect of stratification on energy and exergy capacities in thermal storage systems", *International Journal of Energy Research*, vol. 28, no. 2, pp. 177–193, 2004.

[31] G. Rosengarten, G. Morrison, and M. Behnia, "A second law approach to characterising thermally stratified hot water storage with application to solar water heaters", *Journal of Solar Energy Engineering*, vol. 121, no. 4, pp. 194–200, 1999.

[32] L. J. Shah and S. Furbo, "Entrance effects in solar storage tanks", *Solar Energy*, vol. 75, no. 4, pp. 337–348, 2003.

[33] V. Panthalookaran, W. Heidemann, and H. Müller-Steinhagen, "A new method of characterization for stratified thermal energy stores", *Solar Energy*, vol. 81, no. 8, pp. 1043–1054, 2007.

[34] R. Huhn, "Beitrag zur thermodynamischen analyse und bewertung von wasserwärmespeichern in energieumwandlungsketten", PhD thesis, Technische Universität Dresden, Germany, 2006.

[35] M. Y. Haller, C. A. Cruickshank, W. Streicher, S. J. Harrison, E. Andersen, and S. Furbo, "Methods to determine stratification efficiency of thermal energy storage processes–review and theoretical comparison", *Solar Energy*, vol. 83, no. 10, pp. 1847–1860, 2009.

[36] A. Castell, M. Medrano, C. Solé, and L. F. Cabeza, "Dimensionless numbers used to characterize stratification in water tanks for discharging at low flow rates", *Renewable Energy*, vol. 35, no. 10, pp. 2192–2199, 2010.

[37] M. Christoffersen, "Demand side management of electric water heater with a photovoltaic system", Master thesis, Univiersity of Agder, 2018.

[38] Smarte strømmålere, [Online]. Available: https://www.kamstrup.com/no-no/products-and-solutions/smart-grid/electricity-meters (Accessed 03/09/2018).

[39] Smart relay 30a - remote control for heavy-load equipment, [Online]. Available: %5Curl%7Bhttps://www.develcoproducts.com/products/smart-relays/smart-relay-30a/%7D (Accessed 04/30/2018).

[40] Squid.link gateway - an extremely flexible iot platform, [Online]. Available: %5Curl%7Bhttps://www.develcoproducts.com/products/gateways/squidlink-gateway/%7D (Accessed 04/30/2018).

[41] REC Group. REC peak energy series specifications, [Online]. Available: https://www.recgroup.com/sites/default/files/documents/ds_rec_peak_energy_series_rev_y_eng.pdf (Accessed 03/12/2018).

[42] APsystems YC500A Datasheet, [Online]. Available: http://usa.apsystems.com/wp-content/uploads/2017/07/APsystems-YC500A-Datasheet-6.13.17.pdf (Accessed 03/09/2018).

[43] Apsystems three-phase ecu-3 (v3), [Online]. Available: http://china.apsystems.com/wp-content/uploads/2015/11/4270601031_APsystems-Three-phase-ECU-3-User-manual-for-V3_Rev3.0_2015-10-19.pdf (Accessed 03/09/2018).

[44] APsystems Monitoring, [Online]. Available: https://usa.apsystems.com/products/monitor/ (Accessed 03/09/2018).

[45] CTC FerroTerm - CTC, [Online]. Available: http://www.ctc.no/product/ctc-ferroterm/ (Accessed 03/09/2018).

[46] NI cDAQ-9174 Specifications - National Instruments, [Online]. Available: http://www.ni.com/pdf/manuals/374045a.pdf (Accessed 03/12/2018).

[47]   NI-9216 - National Instruments, [Online]. Available: http : / / www . ni . com / en - no / support/model.ni-9216.html (Accessed 03/12/2018).

[48]   NI-9474 - National Instruments, [Online]. Available: http : / / www . ni . com / en - no / support/model.ni-9474.html (Accessed 03/12/2018).

[49]   Weidmuller Connect Power PRO-E Switch-Mode Power Supplies, [Online]. Available: https : / / www . elfadistrelec . no / Web / Downloads / _t / ds / CP%5C%20E%5C%20SNT_ eng_tds.pdf (Accessed 03/12/2018).

[50]   NI-9212 - National Instruments, [Online]. Available: http : / / www . ni . com / en - no / support/model.ni-9212.html (Accessed 03/12/2018).

[51]   lenovo thinkcentre m710t (10M90007MT for bedrift | Atea eShop, [Online]. Available: https://www.atea.no/eshop/product/lenovo-thinkcentre-m710t-10m9/?prodid= 3586185 (Accessed 03/12/2018).

[52]   Schneider Electric. (2010). Pt100 temperature sensors, [Online]. Available: http://www2. schneider - electric . com / resources / sites / SCHNEIDER_ELECTRIC / content / live / FAQS/239000/FA239836/ru_RU/5pt100sensoren_e.pdf (Accessed 10/23/2017).

[53]   RS Pro PT100 Sensor, [Online]. Available: https : / / no . rs - online . com / web / p / platinum-resistance-temperature-sensors/5477663 (Accessed 03/12/2018).

[54]   Burkert solenoid valve 140850, [Online]. Available: https://no.rs-online.com/web/p/ solenoid-valves/3700107/ (Accessed 03/12/2018).

[55]   GreenTeg flux sensor - gSkin-XM, [Online]. Available: https : / / shop . greenteg . com / shop/heat-flux-measurement/heat-flux-sensor-gskin-xm/ (Accessed 03/12/2018).

Appendix A Physical Setup

This appendix have been written in collaboration with Marius Christoffersen as part of his masters thesis at UiA[37].

In this appendix the system components for making the physical system and conducting experiments. The information for each component is presented in a compressed form, and the information is collected for the manufacturer of each component.

A.1 Advance Metering System

The advanced metering system, AMS is manufactured by Kamstrup and is a 3-phase model. This unit can provide both the customer and grid-operator with information about voltage, events and load profiles. Besides, the unit supports the most common communications interfaces and is ready to use with Home Area Management, HAN-interface[38]. From NVEs description of the HAN-interface, the information from the AMS should include instant power demand, power (active/reactive), current, voltage, energy(active/reactive) and time stamp[**Brev20:online**].

Figure 15 – AMS from Kamstrup[38]

A.2 Power Relays

The system is installed with two separate power relays delivered by E2U. The reason for the relays is to monitor the consumption by the heating element, and the production from the PV system. The data is used for comparing with other collected data. Figure 16 shows one of the relays used. The relays communicate with the gateway using ZigBee communication protocols. In addition to power monitoring, the relays may be used as switches if connected to a cloud service.
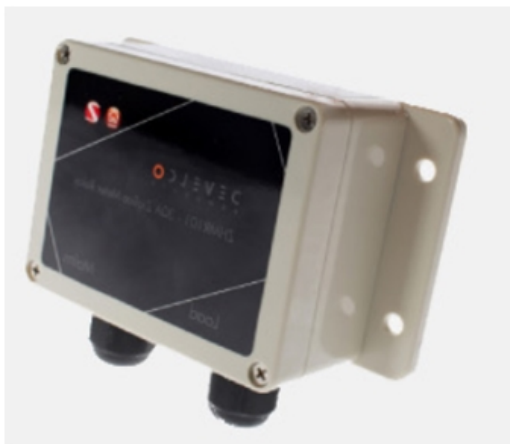
Figure 16 – Develco power relay used for power monitoring of PV and heating element[39]

A.3   Gateway

The gateway is used for communicating with the relays using Zigbee interface. In this system, the gateway is used to communicate with the AMS using the communication port. For communicating with the computer, the gateway uses an ethernet cable with JSON-string interface.

Figure 17 – Gateway for communication between AMS, relay and computer[40]

A.4   PV system

In this appendix the PV system used is presented. Appendix A.4.1 covers the solar panels used, appendix A.4.2 describes the micro inverters and appendix A.4.3 explains the energy communication unit used.

A.4.1   Solar panels

REC group manufactures the solar panels used. For this system, four panels are mounted on the roof at UiA Campus Grimstad, Norway. Combined, the panels has a max peak of 1000W, 250W each[41]. Each panel has an efficiency of 16.7%. Figure 18 shows on the panels mounted.

Figure 18 – Picture of one of the solar panels used

A.4.2   Micro Inverter

In this system there are two micro inverters named YC500A are mounted underneath the solar panels. Each inverter has a maximum output of 500 W and can accommodate 2 PV modules up to 365 W each. Figure 19 is a picture of the inverter. [42]

Figure 19 – Micro inverter from APS[42]

A.4.3   Energy Communication Unit

The APS ECU(Energy Communication Unit) is a user-friendly gateway for the inverters. The ECU provides easy access data for all the connected panels with individual statistics of temperature, voltage and production. In this system, the unit communicates with a computer, using an ethernet cable[43] with updates on changes of production every 5 minutes.

Figure 20 – Energy communication unit from APS[44]

A.5   Electrical Water Heater

The electrical water heater used is a FerroTerm 200-s which with a rated capacity of 194 litres. This tank is delivered with a heating element with a rated power of 1.95 kW and is controlled with a solid state relay. Compared to others manufactures CTC has thicker isolation to reduce heat loss to the environment. Also, the heating element is tilted to ensure heating all the way from the bottom of the tank[45].

Figure 21 – Electrical water heater from CTC[45]

A.6 Data Acquisition System

The data acquisition system has four modules which are arranged in a USB chassis. All the components are from National instruments and are described in detail further below.

USB-Chassis

National Instruments has developed a compact USB-chassis for use with different of the modules available. For this system an NI cDAQ-9174, 4-slots chassis is used which communicating with the computer using USB. The chassis is capable of fast measuring and has high resolution[46]. Figure 22 shows the module.

Figure 22 – Picture of NI cDAQ-9174[46]
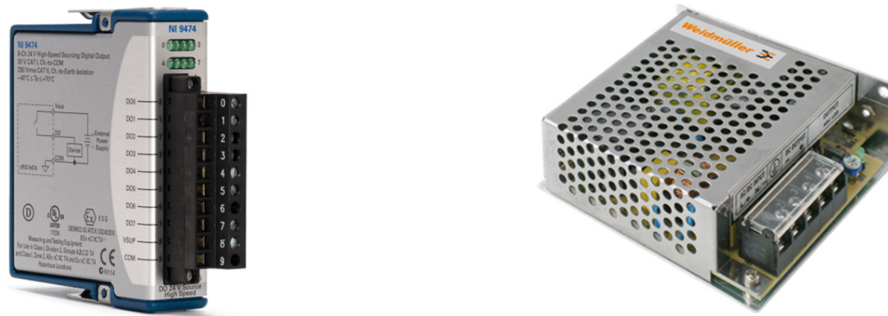
Temperature Module

For collecting information from the temperature devices, a temperature module named NI-9216 from National Instruments is used. This module is designed for use with RTD and is compatible with both 3-wire and 4-wire connections. In this system,, 3-wire is used[47]. Figure 23 presents the module used.
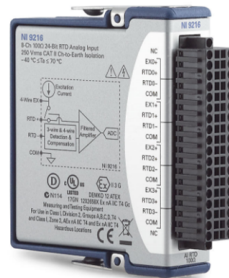
Figure 23 – Temperature module NI-9216[47]

Voltage output module

For controlling the valve in the system, a voltage module named NI-9474 is used, illustrated in figure 24a. This is a voltage output module which works with a wide range of components. For creating controlling signal to control the system relays for valve and heating element control. A 12V DC power supply is used, showed in figure 24b.

(a) Voltage input module NI-9474[48]

(b) 12v DC power supply for valve controller[49]

Figure 24 – Voltage system for valve control

Flux Module

For measuring flux in the system, a temperature module is used. National Instruments has a module called NI-9212 which is designed for thermocouple temperature sensors. In this system, it is used to measure the proportional heat flux from the tank[50].

Figure 25 – Flux module NI-9212[50]

A.7   Computer

The computer used is a Lenovo ThinkCentre M710t. The processor used is a an intel Core I5 and is ideal for use with measurements. The computer is located at UiA and is only used for this experiments[51].

Figure 26 – Lenovo ThinkCentre M710t[51]

A.8   Temperature Sensors

There are five temperature sensors connected to the tank. Three that measure the temperature inside at different heights. Also, a sensor measuring the inlet water temperature, and one measure the outlet temperature. Finally, a PT-100 element is installed outside the tank to measure the room temperature. All the sensors are resistance temperature detectors (RTD) PT100-elements. The sensor is based on the resistance being 100 Ω at $T = 0°C$. Variation in resistance is a function of temperature, approximately 0.39 $\Omega/1°C$ [52]. The connection of PT100-elements varies between 2,3 and 4-wire connection. A 2-wire connection requires calibration due to resistance in the cables. In 3-wire connection, the extra wire functions as a calibration for line resistance, as long as the three wires have the same resistance. For a 4-wire connection, the error from the line resistance is eliminated. This is the most accurate method but is expensive compared to 3-wire systems. In this experiment the type of the connection is 3-wire.

Figure 27 – PT-100 element as mounted on the inlet[53]

A.9 Valve

The valve used to control the water use by regulating the water discharge is a solenoid valve. By applying a voltage through the solenoid, the valve opens or close depending on the configuration. The valve used in this experiment is a normally closed (NC) valve, which means the valve only opens when a voltage is applied. To control the valve a solid state relay (SSR) is used. The relay makes it possible to use the low voltage signal to control large current systems.

Figure 28 – Solinoid Valve[54]

A.10 Heat Flux Sensor

The heat flux sensors used is from greenTEG and of the type gSkin-XM. Two heat flux sensors are used mounted on the outside of the tank at the same height as two of the temperature sensors. That way the temperature inside the tank and in the room can be used as reference temperatures for the sensors. The sensor outputs a voltage to the NI-module, and the voltage can then be used to calculate the heat flux in W/m^2 as,

$$\phi = \frac{U}{S},$$

where ϕ is the heat flux, U is the voltage and S is the total sensitivity given as,

$$S = S_o + \left(\frac{T_h - T_c}{2} - T_0\right) S_c,$$

where S_o is the sensitivity at calibration temperature, T_h and T_c is the temperature on the hot and cold side of the wall respectively, T_0 is the calibration temperature and S_c is the linear correction factor.

Figure 29 – GreenTeg Flux sensor[55]

Appendix B   Average flow calculations

This appendix have been written in collaboration with Marius Christoffersen as part of his masters thesis at UiA[37].
The flow-rate is found by opening and closing the valve at a controlled time interval of 3 seconds and measuring the water discharge from the tank. The average is calculated to be 0.36 liters/s. However, this may not be the correct for all the discharges due to other water usages at the university.

Table 3 – Experiments for calculating system

Opening time valve = 3 seconds		
Test 1	1.055	Liter
Test 2	1.091	Liter
Test 3	1.081	Liter
Test 4	1.1	Liter
Test 5	1.096	Liter
Test 6	1.08	Liter
Test 7	1.068	Liter
Test 8	1.084	Liter
Test 9	1.069	Liter
Test 10	1.08	Liter
Average flow	0.36	Liters/second